Electron Density Study of Garnets: $Z_3Ga_5O_{12}$; Z = Nd, Sm, Gd, Tb

Haruo Sawada

Department of Applied Chemistry, Kogakuin University, 2665-1 Nakano-machi, Hachioji, Tokyo 192, Japan

The electron density distribution in garnets, $Z_3Ga_5O_{12}$, Z = Nd, Sm, Gd, Tb, has been studied with single-crystal X-ray diffraction methods through scattering factor refinement procedures. The Z site shows a variety of electron density residual distribution modes, implying contribution of the f electrons. Residual electron density regions of 0.9–4.0 $e/Å^3$ height seen for all four garnets at an interstitial site (Wyckoff position $48\,g$) suggest coexistence of domains with alternatively oriented structural motifs within the single crystals. [Cubic $Ia\bar{3}d$; a = 12.5051(4) Å (Z = Nd), a = 12.4361(3) Å (Z = Sm), a = 12.3829 (5) Å (Z = Gd), a = 12.3474(5) Å (Z = Tb), final R after anharmonic refinement: Z = Nd, 0.0114 (for 660 equivalent-averaged data); Z = Sm, 0.0111 (647); Z = Gd, 0.0152 (428); Z = Tb, 0.0118 (454).] © 1997 Academic Press

INTRODUCTION

It has been quite a while since the numerous garnet-structured compounds first attracted much attention from various standpoints. The crystal structure of garnets was first determined by Menzer (1, 2). Extensive, collective works on the crystal chemistry of garnets can be found in (3, 4). While there are still growing requirements for especially the synthetic rare-earth varieties for various technological applications, garnets can be considered as yet an unexplored structure type from the viewpoint of studying the accurate electron density distribution. A detailed study on the electron density distribution in these compounds is thus believed to be worthwhile from a wide scope of interest; for instance, from the role of the natural varieties as a composition material of the earth's mantle, to improving the efficiency of the synthetic garnets exhibiting laser qualities.

The difficulties encountered upon precision crystal structure refinement of garnets are believed to arise from factors such as the large differences often seen in the scattering powers of the constituents, and the large number of non-extinct reflections and structural parameters compared to other high-symmetry oxide structures such as spinels, due to the oxygen site of garnet being in the general position. For the present study, intensity data will be processed with rather strict statistics in order to assure reliable structure factor values. Furthermore, a novel method in refining the scattering angle-dependent scattering factors for each atomic site will be incorporated.

The procedure of scattering factor refinement by introducing scattering angle dependency to the occupational parameter has been applied in previous works on corundum-structured sesquioxides (5–7) and spinel-type compounds (8–11). Garnets provide interesting testing grounds for this procedure, since a variety of atomic sites can be compared within one crystal structure.

A generalized formula for garnet $Z_3X_2T_3O_{12}$ is used for notation of the sites, Z at the eight-fold, X at the six-fold, and T at the four-fold coordinated cation sites; Wyckoff positions $24\,c$, $16\,a$, and $24\,d$, respectively. For the present study; X, T = Ga. The Z = Nd species will be denoted NGG; Z = Sm, SGG, Z = Gd, GGG; and Z = Tb, TGG.

EXPERIMENTAL

Specimens cut from wafers synthesized by SHIN-ETSU for use as substrates (NGG, SGG, and GGG), and a rod synthesized by LITTON/AIRTRON for optical use (TGG) were rounded into spheres. The pure compositions were assumed. Cell dimensions were determined from the twenty-four equivalents of the 16 16 8 reflection using graphite-monochromated $MoK\alpha_1$ radiation (0.70926 Å) with a RIGAKU AFC5 automated four-circle diffractometer (40 kV, 30 mA). Intensity data were collected with $MoK\alpha$ radiation (0.7017 Å) with the $2\theta-\omega$ scan. Equivalent reflections were generated within $|h|, |k|, |l| \leq 32$, $2\theta \leq 140°$, $\sin \theta/\lambda \leq 1.322$ from initially measured independent reflections observed with $|F_0| > 6\sigma(F_0)$ (7 in addition for $h\,h\,h$ reflections, 5 additional for others). Those with all additionally measured equivalents observed with $|F_0| > 6\sigma(F_0)$ were averaged into the finally used number of independent data. Various experimental conditions are listed in Table 1. ψ-scan checks made for several strong reflections did not indicate statistically significant fluctuation of intensity suggesting effects of multiple reflection.

TABLE 1
Experimental Conditions for the Four Samples

	NGG	SGG	GGG	TGG
Crystal diameter (mm)	0.26	0.18	0.10	0.19
2θ value of 16 16 8 (°)	85.78	86.38	86.84	87.15
a (Å)	12.5051(4)	12.4361(3)	12.3829(5)	12.3474(5)
D_x (g/cm³)^a	6.612	6.850	7.083	7.180
F 000	3348	3496	3544	3568
μ (/cm)	292.86	319.15	347.58	366.18
Scan width: $a + b\tan\theta$ in ω (°)				
a	1.5	1.45	1.45	1.63
b	0.3	0.35	0.35	0.35
Speed/min in ω (deg)	16	8	4	8
Max. number of repeats	10	10	10	10
Repeated until $|F_o| >$	$200\sigma(F_o)$	$200\sigma(F_o)$	$20\sigma(F_o)$	$20\sigma(F_o)$
Initially measured independents				
Measured	1822	1760	1613	1420
Observed	784	829	632	624
Initially observed (+)				
Generated equivalents	4349	4407	3035	3389
Used to average	3720	3882	2474	2696
Used independent data	660	647	428	454
R_{int}	0.0116	0.0124	0.0176	0.0136
Harmonic refinement:				
Number of scattering factor refinement iterations	38	4	4	5
R	0.0132	0.0123	0.0176	0.0138
R_w	0.0135	0.0134	0.0196	0.0149
Anharmonic refinement:				
Number of scattering factor	6	0	0	3
Refinement iterations				
R	0.0114	0.0111	0.0152	0.0118
R_w	0.0119	0.0116	0.0171	0.0131
Refinement of the occupancy of the $48\,g$ site:				
Occupancy (%)	0.46(6)	0.32(4)	0.16(2)	0.64(9)
R	0.0108	0.0105	0.0152	0.0111
R_w	0.0113	0.0110	0.0169	0.0121

^{a} The values for NGG, SGG, and GGG agree with those in the specifications of these crystals to within 0.02 g/cm³. Data for TGG were not immediately available.

The crystal structure was refined with a modified version of the program RADY (12) applying Lp, absorption, and isotropic extinction corrections, using scattering factors from (13, 14) and dispersion correction values (15). Weights proportional to the theoretical number of equivalents for each reflection were allotted.

The experimental scattering factors for each structure were derived after convergence of the conventional least-squares by refining the occupation parameter g of the site atoms for 11 $\sin\theta/\lambda$ intervals [boundaries: (0.0), 0.3, 0.4, 0.5, 0.6, 0.7, 0.8, 0.9, 1.0, 1.1, 1.2 (1.49)], keeping all other parameters fixed to the old values. The new g values for $\sin\theta/\lambda$ intervals of 0.01 were obtained from interpolation (extrapolation for low- and high-angle regions without observations). Refined g values representing the median $\sin\theta/\lambda$ point in each interval were linearly connected without any smoothing operation.[1] The new scattering factor S for an increment of 0.01 for $\sin\theta/\lambda$ for each site atom was derived from

$$S_j = S_j^o * (g_j/g_j^o) * (e^o/e),$$

$$j = 1\text{--}150 \text{ for } \sin\theta/\lambda = 0.00\text{--}1.49,$$

where the old values have the superscript ^{o}. For the ith atom with n_i atoms contained in the formula, $e = \sum n_i P_i$,

---

[1] There was no significant improvement in the results for structure refinement using scattering factors derived with nonlinear interpolation. In fact, in some cases, use of scattering factors obtained from smoothened g's caused the refinement to veer off to implausible values. An improved version of a smoothing routine is presently under consideration.

with P_i equal to the average scattering factor for a high-angle range $\sin \theta / \lambda = 1.0-1.4$. This measure was taken in order to keep constant the high-angle scattering factor values, which generally do not vary significantly with different ionic states of the same element [13, 14]. This procedure was carried out alternately with the conventional refinement until minimum R was attained. Anharmonic refinement with Gram–Charlier series-expanded parameters up to the sixth-rank tensors (symmetry restrictions taken from [16]) was run next, moving all parameters simultaneously for NGG, SGG, and TGG; only the anharmonic parameters for GGG were varied due to strong correlations with the harmonic parameters. Scattering factor refinement with anharmonic parameters could be run for NGG and TGG, while the results for SGG were not adopted, since correlative movements of the refined scattering factors with the thermal parameters were seen.

DISCUSSION

The cell constants for NGG, SGG, and GGG obtained in the present study agree with those reported previously [17, 18]. As with the cell constants, the $Z-O$ distances (Table 2) for these garnets show a smooth decrease with increase of the atomic number of the Z site ion, a trend consistent with the lanthanide contraction. Refinement with anharmonic parameters in NGG, SGG, and TGG slightly affects the $Z-O'$ and $X-O$ distances, the former becoming nearer and the latter farther.

TABLE 2
List of the Values for the Variable Positional Parameters[2] for Oxygen, and the Nearest Cation–Anion Distances

	NGG	SGG	GGG	TGG
Harmonic refinement				
O: x	0.0300(1)	0.0292(1)	0.0289(2)	0.0282(2)
y	0.0522(1)	0.0530(1)	0.0542(2)	0.0547(2)
z	0.6485(1)	0.6490(1)	0.6494(2)	0.6495(2)
$T-O$(Å)	1.857(1)	1.852(1)	1.848(3)	1.851(2)
$Z-O$	2.407(1)	2.385(1)	2.374(3)	2.361(2)
$Z-O'$	2.520(1)	2.495(1)	2.470(3)	2.455(2)
$X-O$	2.004(1)	2.000(1)	2.001(3)	1.996(2)
Anharmonic refinement				
O: x	0.0296(3)	0.0296(3)		0.0271(6)
y	0.0529(1)	0.0537(3)		0.0553(6)
z	0.6490(3)	0.6490(3)		0.6508(6)
$T-O$(Å)	1.859(4)	1.852(4)		1.852(7)
$Z-O$	2.403(4)	2.392(4)		2.344(7)
$Z-O'$	2.510(4)	2.487(4)		2.449(7)
$X-O$	2.012(4)	2.003(4)		2.011(7)

Note. Estimated standard deviations of last digit are in parentheses.

The differences between the derived and theoretical scattering factors for the four garnets (Fig. 1) show that within the reliable $\sin \theta / \lambda$ range, the corresponding sites have similar patterns, especially for those between NGG and SGG, indicating that in these crystals, the manner in which the refined scattering factors deviate from the theoretical values is essential for each atomic species occupying the sites.

Difference Fourier synthesis of a plane passing through the T and Z sites (Fig. 2) demonstrates the function of the scattering factor refinement procedure; compared to the conventional refinement, concentric rippled features around the atomic positions are removed due to non-Gaussian adjustments made to the theoretical scattering factors, leaving the intrinsically aspherical features intact. For the harmonic scattering factor refinements of NGG and SGG, residuals remain around the Z site, $0.8-1.6$ $e/\text{Å}^3$ in height at about 0.5 Å distance from the Z-site center directed toward four approximately planar-coordinated O sites consisting of unshared edges (corresponding to the far $Z-O'$ distances in Table 2), and perpendicular to this pseudo-plane toward two edges shared with TO_4 tetrahedra. For GGG, the ZO_8 coordination shows positive residuals of ~ 2 $e/\text{Å}^3$ height extending in directions between the planar-coordinated oxygens. There are no peaks seen in this plane for TGG, which shows residuals ~ 1 $e/\text{Å}^3$ in height directed toward edges shared with TO_4.[2]

The diversity of the electron density distribution seen here is implicative of the contributions from the f electrons [19, 20], since the only difference in the electron configuration of the trivalent Z site constituents is the number of f electrons. For Nd^{3+} in NGG and Sm^{3+} (SGG) there are three and five f electrons respectively, against seven f orbitals. The f orbitals are all half-filled for Gd^{3+} (GGG), while one orbital has paired electrons in Tb^{3+} (TGG). It may be conjectured from the various modes of arrangements seen for residuals—axial in TGG, axial $(+)$ [planar, toward oxygens] in NGG and SGG, and [planar, avoiding oxygens] in GGG, with the axis perpendicular to the (pseudo-)plane—that the quantization axis should coincide with the TGG residual direction, which would correspond to the paired electrons in the orbital having a wavefunction with the angular part $z(5z^2 - 3r^2)$ [19, 20]. Two electrons in the half-filled planar orbitals in

[2] See NAPS documents for supplementary material; No. 5411 for NGG (61 pages), No. 5412 for SGG (49 pages), No. 5413 for GGG (49 pages), No. 5414 for TGG (50 pages). These are not multi-article documents. Order from NAPS c/o Microfiche Publications, P.O. Box 3513, Grand Central Station, New York, NY 10163-3513. Remit in advance in U.S. funds only $7.75 for photocopies or $5.00 for microfiche. There is a $15.00 invoicing charge on all orders filled before payment. Outside U.S. and Canada add postage of $4.50 for the first 20 pages and $1.00 for each 10 pages of material thereafter, or $1.75 for the first microfiche and $0.50 for each microfiche thereafter.
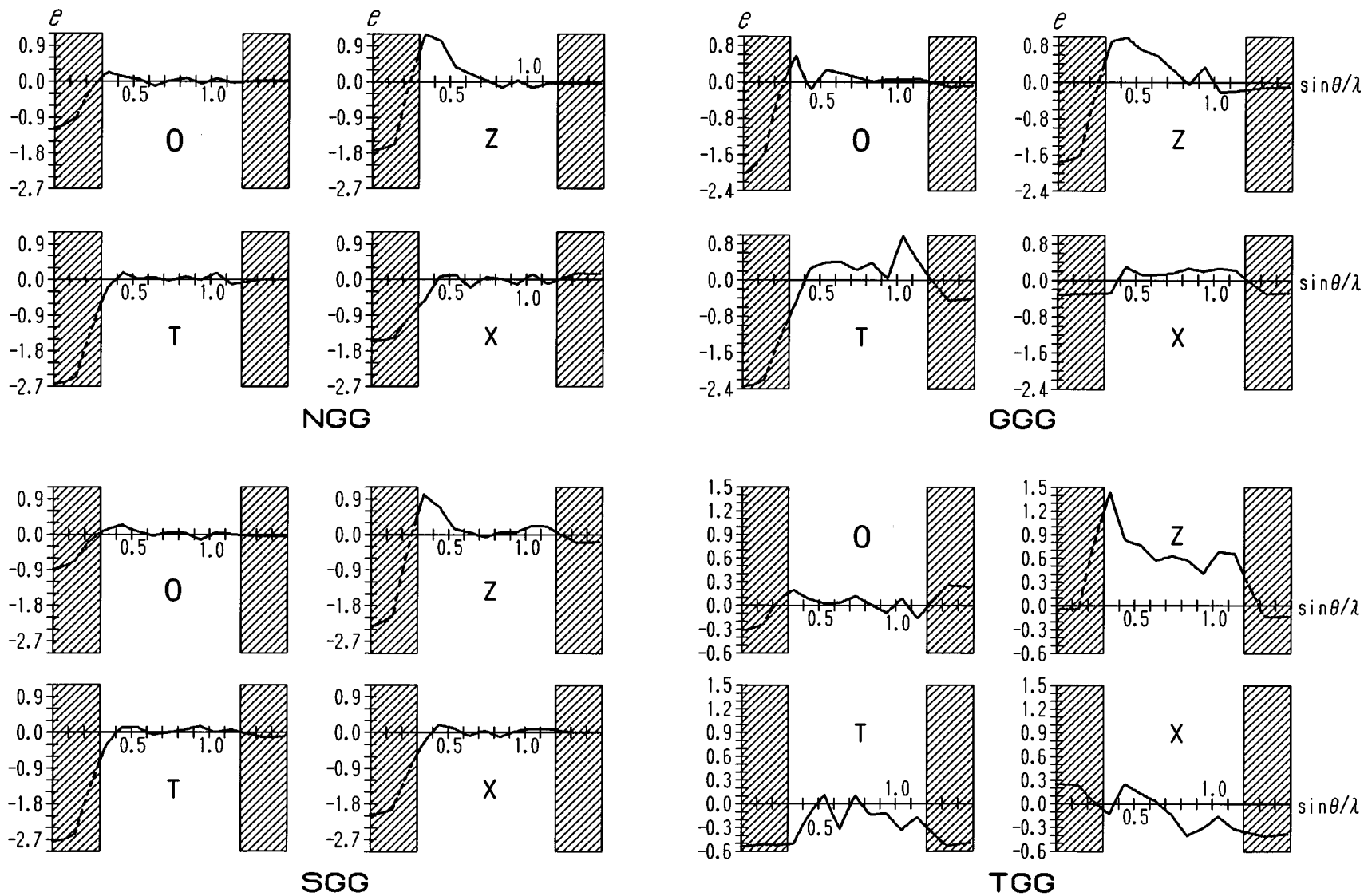
FIG. 1. The theoretical scattering factors subtracted from those derived (see footnote 2) from scattering factor refinement with the harmonic parameters. The $\sin\theta/\lambda$ range outside the fully interpolated region is shown hatched.
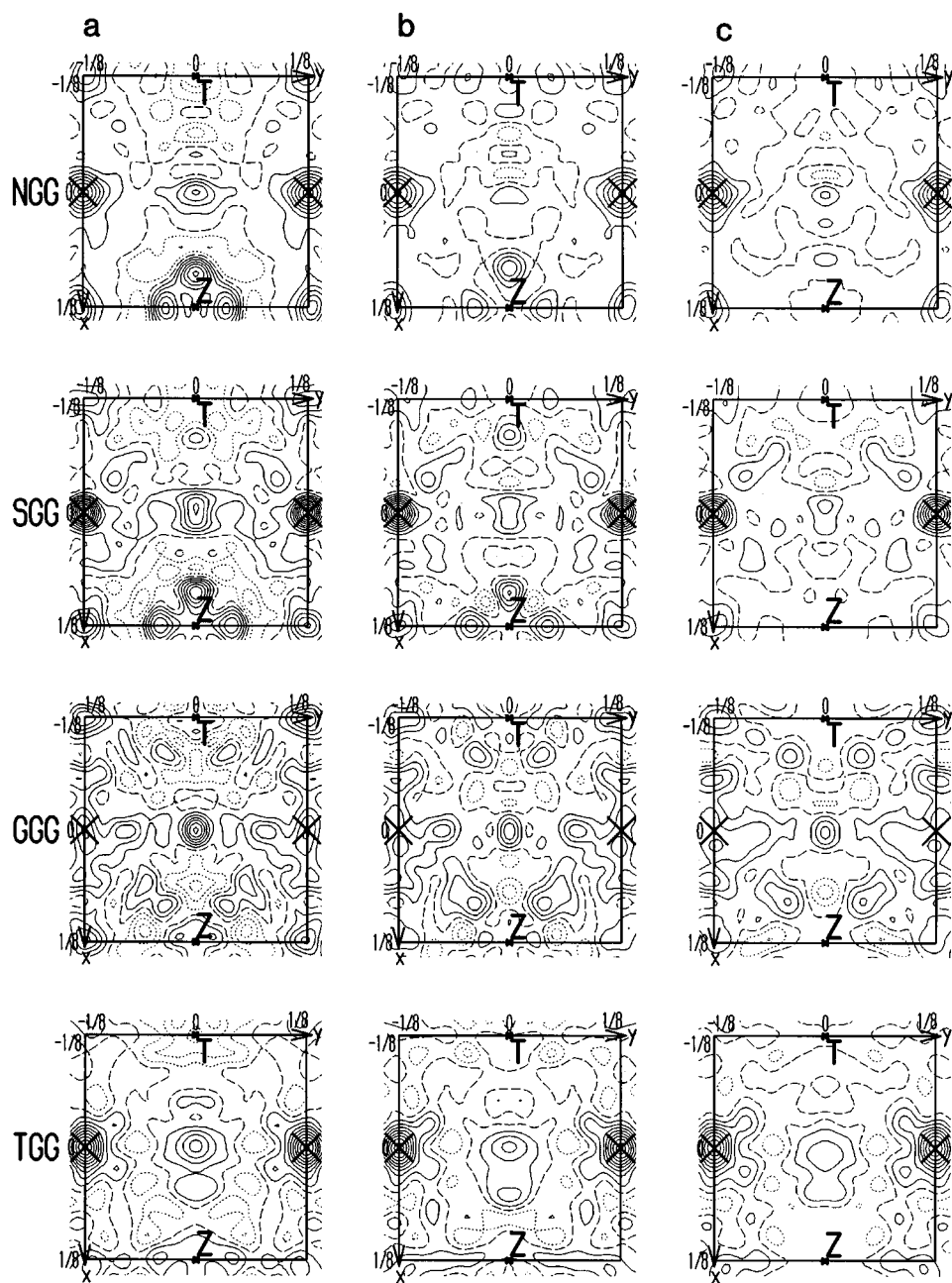
FIG. 2. Difference Fourier sections (see footnote 2) for plane $z = 1/4$ passing through the T and Z sites. Large crosses indicate the $48g$ site peak position. Positive contours are shown in solid lines, zero contours in broken lines, and negative contours in dotted lines with increments of 0.4 $e/\text{Å}^3$: (a) Conventional harmonic refinement, and (b) harmonic and (c) anharmonic scattering factor refinements.

NGG and SGG, which would correspond to the $x(x^2 - 3y^2)$ and $y(y^2 - 3x^2)$ wavefunctions, appear to be participating in bonding. In Sm^{3+}, although two more electrons must occupy two of the remaining four orbitals with mixed angular contributions of x, y, and z components for a high-spin-type filling up of the f orbitals, this cannot be verified from the distribution of the residuals in SGG. However, the

higher peak heights compared to that of the corresponding residuals in NGG indicate that the remaining two electrons in Sm^{3+} are also distributed in orbital lobes more or less overlapping with the first three. Meanwhile, without a major breakdown in the energy degeneracy for the $4f$ levels of Gd^{3+}, the residuals seen in GGG may be attributed rather to the nonbonding electrons, since they are arranged

so as to avoid the oxygens. This argument is, of course, subjected to adjustments when factors such as significant configuration mixing with other electronic states or hybridization of the orbitals must be taken into consideration. However, the form of the Z site, which is considerably distorted from any polygon or idealized polyhedron, brings about a sense of irresoluteness in attempting to theoretically deduce the spatial distribution of the f electrons around this site.

Another point worth mentioning is that the angular distributions of atomic orbitals generally have much in common with the directions that the anharmonic parameters represent, so it may be impossible to distinguish clearly between statistically deformed and anharmonically vibrating atoms. Some of the residuals seen around the Z site mentioned above are completely removed by introduction of anharmonic parameters. Previous studies on the first-row transition element compounds $(6, 7, 10)$ gave similar results; in the harmonic refinement, residuals suggesting the distribution of $3d$ electrons were detected, which almost completely disappeared after anharmonic refinement. In the present case, the relatively large distances of the residuals from the nucleus are believed to give some support to the static deformation scheme.

A striking feature common to all modes of refinement in these garnets (Fig. 2) is a strong positive residual centered on an interstitial site at Wyckoff position $48\,g$; variable parameter $y = 1/4$ for the expression in (21). The residual heights are, for NGG, 2.5–3.0; for SGG, 3.1–4.0; for GGG, 0.9–1.6; and for TGG, 3.2–3.7 $e/\text{Å}^3$. The shape of this residual is a rather diffused plateau in GGG, while those for the other three garnets are close to symmetrical peaks, which appear more or less like miniature Fourier peaks of atoms.

It should be noted that this position has only a diad axis, and along with the $48\,f$ position, it is the special position of lowest symmetry in this space group. Accumulation of various errors would thus be expected to occur generally with greater severity at the other special positions having higher symmetry.

Comprehension of the nature of this residual peak may be initiated by noting that in the garnet structure, only half of the 96 positions with the following fractional coordinates are occupied by Ga at $24\,d$ or the Z site ion at the $24\,c$ position

$$[(n_1/8,\ n_2/4,\ n_3/2); \qquad n_1 = 1, 3, 5, 7;$$

$$n_2 = 1, 3;\ n_3 = 0, 1;\ \text{coordinates permutable}],$$

the remaining unoccupied half being the $48\,g$ positions. The symmetries of these positions depend on the permutation of the crystallographic axes and the coordinates; therefore, a minor fraction of this garnet crystal assuming an orientation corresponding to a different choice of axes would be observed from the major orientation as having these atoms situated at normally unoccupied sites, i.e., the $48\,g$ positions.

Consequently, in the present case, the alternative orientation can be defined either as a right-angled rotation around a coordinate axis or as twinning on the (110) planes. Lack of mirror symmetry in this space group adds to the complexity by bringing about a possibility of an atomic arrangement pertaining to a left-handed coordinate system. The X site, however, invariant to these operations. The fraction of electron densities changing position from the T and Z sites shows up superpositioned at the $48\,g$ site. The O site, which is at the general position, shifts to several different sets of equivalent positions when viewed from the original coordinate system. Due to this, and the comparatively small scattering power and large thermal vibrations, the occupation of alternative sites by oxygen is supposedly undetectable in the present study.

Examination of Fig. 3 shows that there is a small positive difference electron density remaining at the X site after scattering factor refinements. Further refinement with anharmonic parameters shows similar results. This seems to give supporting evidence to the occurrence of partial migration of atoms from the Z, T, and O sites; since the scattering powers are more or less adjusted to these sites which have the majority of the total number of electrons, the actually unchanged X site shows increase of electron density.

Refinement of the occupancy of the $48\,g$ site, using mean values of T and Z for the scattering factors and isotropic temperature factor (fixed) starting from the harmonically refined scattering factors and the anharmonically refined parameters, yields occupation of less than 1% of the total number of T and Z atoms for all four garnets (Table 1). The features seen in the difference Fourier maps are practically identical to those in the anharmonic run except for the $48\,g$ site, where the positive peak was mostly removed (see footnote 2).

Considering the above result that the alternative orientation seems to take place only with minor proportions, it follows that this situation has likely arisen solely from the boundary regions of domains with differently oriented motifs. Since garnet (thus, each domain) is centrosymmetric cubic, a large part of domains which are much larger than the limiting volume of coherent diffraction would behave under X-ray diffraction as indistinguishable single crystals regardless of their orientations (parallel to, or in right angles to each other) or handedness. On the other hand, interference between diffracted beams emitted from domains with differently oriented motifs can occur within the confinement of diffraction coherence in the proximity of the boundaries, affecting the overall diffraction intensities to a certain extent, thus exhibiting the $48\,g$ site residuals upon difference Fourier synthesis with these intensity data. Therefore the above "occupation" of the $48\,g$ site may serve as an indicator to the ratio between the extent of the region of
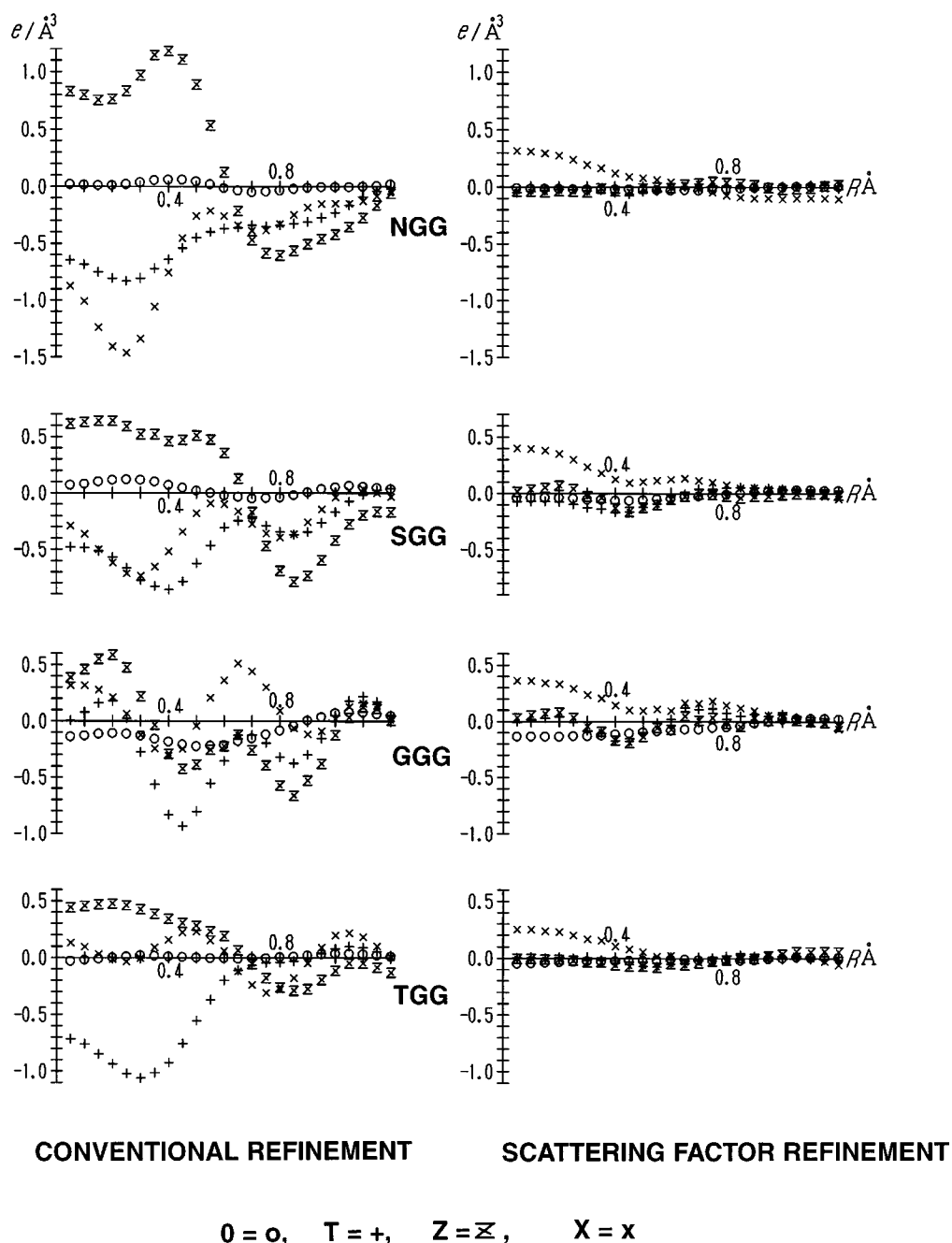
FIG. 3. The average residual electron density within spherical shells of radius $(R - 0.05) \sim R$ Å around the atomic sites for refinement with harmonic parameters.

interferences and the remaining volume of the domain with a uniform structural motif displaying no interference.

Some natural garnets displaying strong optical anisotropy in fact have noncubic structure and can frequently become twinned (22). The present case differs in that each of the domains are of cubic symmetry with an ideal garnet structure, the discriminating factor being in their motifs. Moreover, the manner of twinning presently encountered may have been realized through reticular merohedry, that is, with preservation of a partial structure common to all orientations, namely, the unaltered X site arrangement.

NGG shows an inexplicable negative residual of $-2.0- -2.8$ $e/$Å^3 height situated at Wyckoff position 16 b

$(1/8, 1/8, 1/8)$, which is the center of the largest interstitial void in the garnet structure, with oxygen coordination of a slightly twisted triangular prism. This residual cannot be seen in the other three garnets, and since no immediate physical meaning is perceived, the possibility is that this residual in NGG is due to accumulation of various errors. Electron density residuals can also be seen remaining in some of the other unoccupied special positions of high point symmetry in these garnets (Fig. 2, see also footnote 2).

Correlations may exist between the motif-domain structure discussed here and the magnetic domain structure in the magnetic garnets. There may also be some effect on delicate spectral properties such as laser efficiency. Reports on investigation of other related garnet structures are in preparation in order to give confirmation to the present results.

ACKNOWLEDGMENTS

REFERENCES

1. G. Menzer, *Z. Kristallogr.* **63,** 157 (1926).
2. G. Menzer, *Z. Kristallogr.* **69,** 300 (1928).
3. G. Geller, *Z. Kristallogr.* **125,** 1 (1967).
4. G. A. Novak and G. V. Gibbs, *Am. Miner.* **56,** 791 (1971).
5. H. Sawada, *Mater. Res. Bull.* **29**(2), 127 (1994).
6. H. Sawada, *Mater. Res. Bull.* **29**(3), 239 (1994).
7. H. Sawada, *Mater. Res. Bull.* **31**(2), 141 (1996).
8. H. Sawada, *Mater. Res. Bull.* **30**(3), 341 (1995).
9. H. Sawada, *Mater. Res. Bull.* **31**(4), 355 (1996); Erratum, *Mater. Res. Bull.* **31**(8), 1045 (1996).
10. H. Sawada, *Mater. Res. Bull.* **31**(4), 361 (1996).
11. H. Sawada, *Mater. Res. Bull.* **31**(4), 367 (1996); Erratum, *Mater. Res. Bull.* **31**(8), 1045 (1996).
12. S. Sasaki, "KEK Internal," Vol. 87-3. National Laboratory for High Energy Physics, Tsukuba, 1987.
13. "International Tables for X-ray Crystallography," Vol. IV. Kynoch Press, Birmingham, 1974.
14. M. Tokonami, *Acta Crystallogr.* **19,** 486 (1965).
15. "International Tables for X-ray Crystallography," Vol. III. Reidel, London, 1983.
16. W. F. Kuhs, *Acta Crystallogr. Sect. A* **40,** 133 (1984).
17. F. Bertaut and F. Forrat, *C. R. Acad. Sci.* (*Paris*) **243,** 1219 (1956).
18. S. J. Schneider, R. S. Roth, and J. L. Waring, *J. Res. Natl. Bur. Stand. Sect. A* **65,** 345 (1961).
19. H. G. Friedman Jr., G. R. Choppin, and D. G. Feuerbacher, *J. Chem. Educ.* **41,** 354 (1964).
20. C. Becker, *J. Chem. Educ.* **41,** 358 (1964).
21. "International Tables for X-ray Crystallography," Vol. A. Kluwer Academic, Dordrecht, 1983.
22. Y. Takéuchi, N. Haga, S. Umizu, and G. Sato, *Z. Kristallogr.* **158,** 53 (1982).